

Quantum rounding

Rajiv Krishnakumar and William J. Zeng

Goldman Sachs & Co.

We introduce new rounding methods to improve the accuracy of finite precision quantum arithmetic. These quantum rounding methods are applicable when multiple samples are being taken from a quantum program. We show how to use multiple samples to stochastically suppress arithmetic error from rounding. We benchmark these methods on the multiplication of fixed-point numbers stored in quantum registers. We show that the gate counts and depths for multiplying to a target accuracy can be reduced by approximately 2-3X over state of the art methods while using roughly the same number of qubits.

1 Introduction

Recent efforts have been made to quantify the resources needed to run potentially commercially relevant quantum algorithms [4, 9, 10, 19]. These algorithms often have subroutines of arithmetic operations. Although these types of subroutines are commonplace and easily implemented on classical computers, they can consume significant resources on quantum computers. This is a problem as the quantum computers of today (and of the near tomorrow) have limited quantum memory and limited quantum coherence. Therefore it is desirable to reduce resources and precision for quantum arithmetic.

In this paper, we propose *quantum rounding* to increase the precision of quantum arithmetic at a fixed quantum register size. These quantum rounding methods are applicable when multiple samples are being taken from a quantum program.

In Section 2 we introduce quantum rounding and give two quantum circuit implementations. Section 3 analyzes the errors in these rounding methods and compares their scaling against traditional rounding approaches. We find for a quantum program in which N samples are taken, the worst-case quantum rounded error is suppressed as approximately $\mathcal{O}(1/\sqrt{N})$. In Appendix A we introduce an alternative *quantum semi-rounding* method whose error we study in an average case analysis.

Section 4 presents the resources needed to scale quantum rounding methods. In Section 5 we compare the resources used for quantum rounding with other methods when applied to fixed-point multiplication with an allowed target error. Figures 3 and 4 show that the gate counts and depths can be reduced by approximately 2-3X over state of the art methods while using roughly the same number of qubits.

2 Quantum Rounding

Finite precision introduces errors. Let $\bar{x} \in \mathbb{R}$ be an exact numerical representation. The n -bit fixed point representation is

$$x = \underbrace{x_{n-1} \cdots x_{n-p}}_p \cdot \underbrace{x_{n-p-1} \cdots x_0}_{n-p}. \quad (1)$$

Rajiv Krishnakumar: rajiv.krishnakumar@gs.com

William J. Zeng: william.zeng@gs.com

Assume that \bar{x} is rational and exactly represented by $n + m$ bits.

$$\bar{x} = \underbrace{\bar{x}_{m+n-1} \cdots \bar{x}_{m+n-p}}_p \cdot \underbrace{\bar{x}_{m+n-p-1} \cdots \bar{x}_m}_{n-p} \underbrace{\bar{x}_{m-1} \cdots \bar{x}_0}_m. \quad (2)$$

We then have a few choices for how to round \bar{x} to x . Truncating by rounding up or down introduces an error $\epsilon_{RD} \leq 1/2^{n-p}$. If we instead round to the nearest n -bit representable number, then our error is $\epsilon_{RN} \leq 1/2^{n-p-1}$.

Recently, demand for high throughput in classical machine learning applications has driven the study of an alternative method called stochastic rounding [5, 12, 20, 27]. Here, one rounds up or down with equal probability each time. Implementing this in practice classically requires access to a reliable and fast source of randomness. On a quantum computer we can do this relatively easily. Let $\lfloor x \rfloor$ and $\lceil x \rceil$ be the rounded down and rounded up n -bit representations of \bar{x} respectively. To stochastically round, we add an additional ancilla qubit and prepare it in the $|+\rangle$ state. We then do an controlled addition of ϵ_{RD} to the rounded down state, where the control is on the value of the $|+\rangle$ state ancilla. This creates the state

$$\frac{1}{\sqrt{2}} (|\lfloor x \rfloor, 0\rangle + |\lceil x \rceil, 1\rangle) = \frac{1}{\sqrt{2}} (|\lfloor x \rfloor, 0\rangle + |\lceil x \rceil, 1\rangle). \quad (3)$$

Measuring the ancilla will probabilistically round up or down with equal probability. The ancilla can then be conditionally reset to $|0\rangle$. In this manner any benefits from stochastic rounding can be naturally obtained in the quantum setting.

However, we can do better by making a specific choice of a non-uniform superposition between rounding up or down. In quantum rounding, we make use of the extra m bits to bias the rounding direction so that the expected value of many roundings converges to the higher precision. Specifically, define the remainder

$$r = \sum_{j=1}^m 2^{-j \cdot \bar{x}_{m-j}} = \frac{\bar{x}_{m-1} \cdots \bar{x}_0}{2^m}. \quad (4)$$

to be the last m bits normalized between zero and one. In this formula we treat $\bar{x}_{m-1} \cdots \bar{x}_0$ as an integer. The remainder r can be interpreted as a probability of rounding up. We then prepare the ancilla in the superposition

$$\sqrt{1-r}|0\rangle + \sqrt{r}|1\rangle \quad (5)$$

and perform the same controlled addition as before. This results in

$$|x\rangle = \sqrt{1-r}|\lfloor x \rfloor, 0\rangle + \sqrt{r}|\lceil x \rceil, 1\rangle. \quad (6)$$

In this final state, the expected value of the main register is exactly \bar{x} . Should this rounding circuit be executed repeatedly, as is commonly the case in quantum programs where multiple samples are taken, the register will converge to the exact value.

2.1 Circuit Construction

Let $|\bar{x}_r\rangle = |\bar{x}_{m-1} \cdots \bar{x}_0\rangle$. In order to prepare the ancilla in the state from (5), we perform an operation

$$|\bar{x}_r\rangle |0\rangle \mapsto |\bar{x}_r\rangle (\sqrt{1-r}|0\rangle + \sqrt{r}|1\rangle). \quad (7)$$

We'll call this phase loading. An example circuit for quantum rounding using this procedure is described in Figure 1 using the controlled rotation loading method of [4]. Here the $|\bar{x}_r\rangle$ register undergoes a square root and then arcsin operation. Controlled rotations are then applied bitwise between this result and another ancilla. Unfortunately this method may be resource expensive as it requires computing a square root and arcsin of a quantum register.

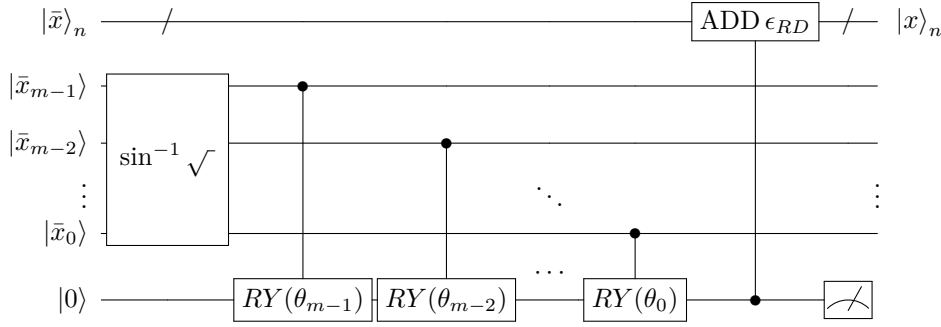


Figure 1: Circuit for quantum rounding an $n + m$ -bit number $|\bar{x}\rangle$ to a n -bit number $|x\rangle_n$. Here $\theta_i = \sin^{-1}(2^{-(m-i)})$. The m -bit register becomes garbage that can be uncomputed. The ancilla can be conditionally reset and reused.

We introduce an alternative method to replace phase loading that is inspired by quantum counting and that reduces the resources used.¹ We first add m ancilla qubits in the uniform superposition.

$$|\bar{x}_r\rangle_m |+\rangle_m = \sum_{j=0}^{2^m-1} \frac{1}{\sqrt{2^m}} |\bar{x}_r\rangle_m |j\rangle_m \quad (8)$$

We then add an additional qubit controlled on the ancilla and apply a comparator circuit [7]. The comparator unitary operations perform

$$\text{Compare} : |a\rangle |b\rangle |0\rangle \mapsto |a\rangle |b\rangle |0\rangle \text{ if } a > b \text{ and } 1 \text{ otherwise}. \quad (9)$$

We can think of the m ancilla qubits as a discretization of the interval $[0, 1]$ into 2^m bins. The comparator is then accumulating into a quantum amplitude an amount $1/\sqrt{2^m}$ for each bin that is less than r . This results in

$$\sum_{j=0}^{2^m-1} \frac{1}{\sqrt{2^m}} |\bar{x}_r\rangle_m |j\rangle_m |j < \bar{x}_r\rangle = |\bar{x}_r\rangle_m \otimes \left[\sum_{j=0}^{\bar{x}_r-1} \frac{1}{\sqrt{2^m}} |j\rangle_m |1\rangle + \sum_{j=\bar{x}_r}^{2^m-1} \frac{1}{\sqrt{2^m}} |j\rangle_m |0\rangle \right]. \quad (10)$$

The probabilities of the comparator ancilla outcomes are now

$$\Pr[\text{ancilla is } 1] = \frac{\bar{x}_r}{2^m} = r \quad (11)$$

$$\Pr[\text{ancilla is } 0] = \frac{2^m - \bar{x}_r}{2^m} = 1 - r. \quad (12)$$

This is precisely what we desire for quantum rounding. Figure 2 gives an example circuit for this approach.

Note that the mid-circuit measurement of the ancilla qubit does not affect the operation of any program that uses quantum rounding as a subroutine as long as the program's output is eventually classical (rather than a quantum state output). To see this, we could not re-use ancillas and instead defer all the mid-circuit measurements to the end of a quantum computation. The results of the final ancilla-rounding measurements can then be thrown away while the results of the computationally relevant measurements are kept.

2.2 Loading rounded classical numbers

When the original number \bar{x} is classical, then the procedure can be simplified. One can use a rotation $RY(\sin^{-1}(\sqrt{r}))$ on the largest remainder bit, but it may be easier to use a purely

¹Versions of this trick were used for different applications in the Hamiltonian time evolution simulation algorithm in [16] and the Coherent Iterative Energy Estimation algorithm of [23].

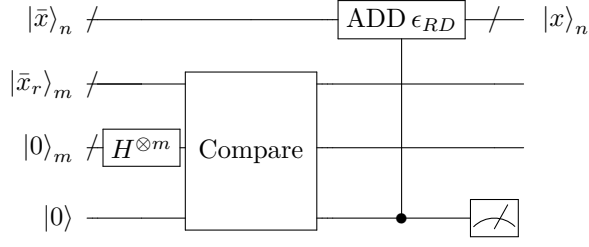


Figure 2: Circuit for quantum rounding an $n + m$ -bit number $|\bar{x}\rangle$ to a n -bit number $|x\rangle_n$ using the comparator method. The m -bit register becomes garbage that can be uncomputed. The ancilla can be conditionally reset and reused.

classical procedure. Instead of deterministically loading \bar{x} , load $\lceil x \rceil$ with probability r and load $\lfloor x \rfloor$ with probability $1 - r$. Sampling either $\lceil x \rceil$ or $\lfloor x \rfloor$ can be done classically. We then gain the advantages of quantum rounding, but use no additional quantum resources.

3 Errors in quantum rounding

We first consider the case where all gates can be implemented exactly e.g. that we are either using the comparator based method (Fig. 2) or the rotation method (Fig. 1) with the assumption that we can apply exact Ry gates. We can use the Chernoff bound to bound the error in the expected value of our register $|x\rangle$.

Theorem 1 (Chernoff). *Let $X = \sum_{i=1}^N X_i$ be a sum of independent Bernoulli random variables X_i that each take the value 1 with probability p_i and the value 0 with probability $1 - p_i$. Let $\mu = \sum_{i=1}^N p_i$ be the mean of X . Then for any choice of $\delta \in (0, 1)$ we obtain*

$$P(|X - \mu| \geq \delta\mu) \leq 2^{-\mu\delta^2/3}. \quad (13)$$

In our setting, X_i is the i -th measurement outcome that is sampled from the rounded state. Then $p_i = r$ and $\mu = Nr$ and the expected error after N samples is bounded by

$$P\left(\frac{|X - Nr|}{N} \geq \delta r\right) \leq 2^{-\mu\delta^2/3}. \quad (14)$$

Setting $\delta = \sqrt{\frac{3 \ln(2/\alpha)}{Nr}}$ gives a failure rate of α that bounds

$$P\left(\frac{|X - Nr|}{N} \geq \sqrt{\frac{3 \ln(2/\alpha)}{N}}\right) \leq \alpha, \quad (15)$$

where we have used the upper bound of $r \in [0, 1]$. In practice it may be reasonable to choose $\alpha = 1/N$ so that a failure is not expected.

After N samples our empirical mean value for the register is

$$x_{QR} = \frac{X}{N}\epsilon_{RD} + \lfloor x \rfloor. \quad (16)$$

Let the true value $\bar{x} = \lfloor x \rfloor + x_R$. Then our error is

$$|x_{QR} - \bar{x}| = \left| \frac{X}{N}\epsilon_{RD} - x_R \right| \quad (17)$$

$$= \left| \frac{X}{N} - \frac{x_R}{\epsilon_{RD}} \right| \epsilon_{RD} \quad (18)$$

$$= \left| \frac{X}{N} - r \right| \epsilon_{RD} \quad (19)$$

$$\leq \epsilon_{RD} \sqrt{\frac{3 \ln(2/\alpha)}{N}} \quad \text{w/ prob. } \geq 1 - \alpha. \quad (20)$$

Comparing to the round-nearest method, we reduce the error by a factor

$$F = \frac{1}{2} \sqrt{\frac{3 \ln(2/\alpha)}{N}}. \quad (21)$$

As N increases, the error compared to the round-nearest method decreases significantly. For $\alpha = 1/N$ and $N \approx 500$ then error is reduced by an order of magnitude. For $\alpha = 1/N$ and $N = 90k$ then error is reduced by two orders of magnitude.

3.1 Rotation errors

If we are using the rotation approach then we should also take into account errors in rotation gates. Rotation errors may be due to approximate synthesis in a fault-tolerant setting or physical gate noise in a NISQ setting. If the errors are unbiased then the Chernoff bounds apply as in the above section since we still have $\mu = \sum_i^N p_i$.

A bias in the rotations will cause additional error. A rotation error that results in an amplitude $\sqrt{r} + \epsilon_{rot}$ results in an error on the probability of $\epsilon_B \leq (\sqrt{r} + \epsilon_{rot})^2 \leq 2\epsilon_{rot} + \epsilon_{rot}^2$. Thus we obtain

$$|x_{QR} - \bar{x}| \leq \epsilon_{RD} \left(\sqrt{\frac{3 \ln(2/\alpha)}{N}} + \epsilon_B \right). \quad (22)$$

4 Resource Estimates

We now consider the resources used to implement quantum rounding circuits. In the fault-tolerant setting we assume that resources are dominated by the T gate count and depth, with the CNOT gate count and depth having a smaller but still non-trivial impact. Therefore we choose to use appropriate circuits that minimize the T-depth whilst still ensuring that our CNOT gate counts and depth do not become exponentially large. A more detailed discussion of the focus on minimizing the T-depth can be found in Section B.1.

Table 1 shows the resources used for a 10-bit representation of \bar{x} along with a 10-bit remainder, i.e. when $n = m = 10$. The method used is the comparator circuit from Figure 2. These tables also show the leading order dependence for generic n and m . Additional resource estimates along with a more detailed explanation of their computations are given in Appendix B.

Table 1: Resources for quantum rounding in a fault-tolerant setting. The rounding circuit used is in Fig.2.

| Resource | $n = m = 10$ | Leading order terms |
|---------------------|--------------|-------------------------------|
| Additional qubits | 12 | m |
| Uncomputed ancillas | 34 | $\max(4m, 3n)$ |
| T-count | 588 | $24m + 30n$ |
| T-depth | 32 | $2 \log_2(m) + 2 \log_2(n)$ |
| CNOT count | 1509 | $62m + 82n$ |
| CNOT depth | 323 | $20 \log_2(m) + 20 \log_2(n)$ |

5 Applications and Benchmarks

For a single rounding step, the error can be exponentially decreased by increasing the rounded register size n . This might appear to be preferable to the overhead of quantum rounding. However, increasing precision means that the rest of the computation must proceed with a larger value of n after that rounded step. If the rest of the computation is long and/or involved then benefits can be found from quantum rounding.

5.1 Fixed point multiplication benchmarks

As an example, we calculate the resources for a fixed-point multiplication in a fault tolerant setting, where several steps of rounding are often used. For a number of samples $N > 1$ quantum rounding will add extra accuracy per rounding step, allowing us to reduce the precision to achieve a target overall accuracy. In our benchmarks we choose $n = m$ for simplicity and choose the target $\epsilon = n/2^{n-p}$ as this is the baseline accuracy from the Haner et al. method from Appendix A in [11].²

In Figure 3 and Figure 4 we compare using three different techniques on n -bit fixed point multiplication. The Exact method is exact multiplication to a $2n$ -bit precision that is then rounded-down to n -bit precision. The Haner et al. [11] method uses fewer qubits per addition and does no rounding since it assumes the worst case error for each addition. A detailed explanation of the implementations of these methods is given in Appendix C. Our quantum rounding method does exact multiplication to $2\tilde{n}$ -bit precision and then quantum rounds down to \tilde{n} -bit precision. Here \tilde{n} is the smallest register size that matches the error target $\epsilon = n/2^{n-p}$ of the other approaches. Generally $\tilde{n} \leq n$ with the difference growing as the number of samples N increases. We calculate resources using the fault-tolerant resource counts for quantum rounding.

Figure 3 compares the different methods for a fixed number of samples $N = 10k$ across different register sizes n . For the gate resources of CNOT and T gate counts and depths, quantum rounding reduces resources by about a factor of 2. However, quantum rounding uses slightly more qubits than Haner et al. (but fewer than the Exact method). This is shown in Figure 3c.

Figure 4 fixes the register size to 10 qubits and varies the number of samples. We see that across the gate metrics more samples rapidly reduce the resources used. This advantage plateaus at about a 3X advantage over the Haner et al. method. We see that the number of qubits used starts worse than the Haner et al. method but becomes comparable for large numbers of samples.

These benchmarks give just one example using fixed-point multiplication. For other subroutines and larger algorithms the optimal tradeoff between qubits, additions, and rounding accuracy will likely vary.

5.2 Other applications

The idea behind quantum rounding can also be applied to floating point representations where we wish to better round between machine representable numbers. Here one could apply quantum rounding methods to the mantissa.

One could also consider approximate versions of quantum rounding. In Appendix A we consider a version of quantum rounding - *quantum semi-rounding* - where only the most significant bit of the remainder is used. This method does not appear to result in a saving over the comparator implementation of quantum rounding due to the resources used just to estimate the most significant bit. There may still be a better method for this approach.

Quantum rounding methods are likely to be particularly relevant in applications of quantum computers to problems that have classical oracles such as in optimization and finance. In those cases the quantum implementation of the arithmetic in the classical oracle can absorb significant resource costs, e.g. in the Quantum Approximate Optimization Algorithm [8] applied to classical objective functions.

6 Acknowledgements

We would like to thank Thomas Häner and Dimitri Maslov for references and suggestions on quantum arithmetic constructions. We thank Patrick Rall and Nikitas Stamatopoulos for helpful discussion and review.

²This method can be described as the binary version of the usual schoolbook multiplication i.e. a series of additions of one number register to a result register controlled on the other number register. However in the original paper, the authors use the addition circuit in [26] when computing the resources for this method of multiplication. We instead modify it slightly by using the addition circuit in [7] which is optimized for T-depth (at the cost of an increase in T-count). Going forward we will refer to this modified version as the Haner et al. method.

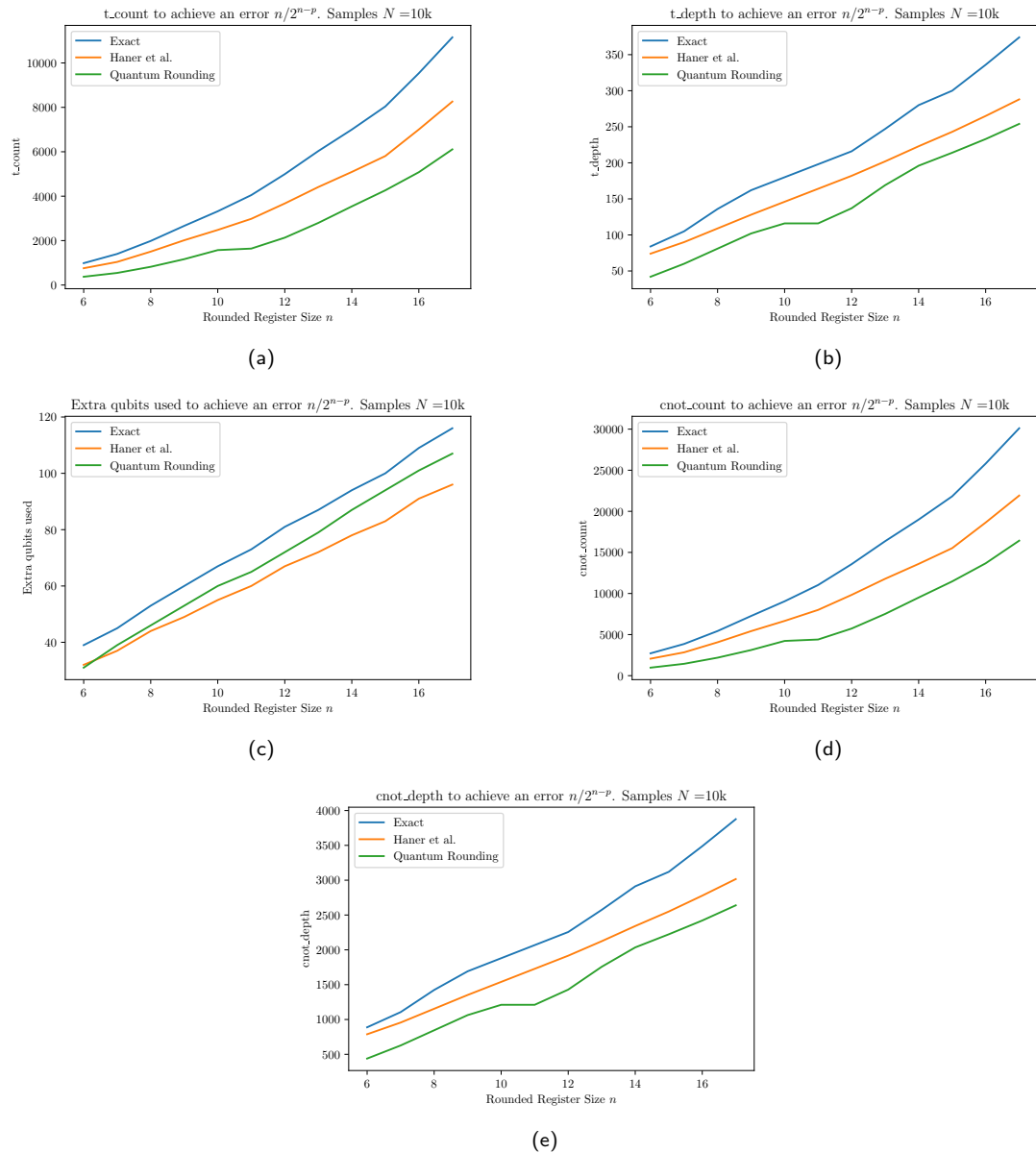


Figure 3: Comparison of different resource metrics for fixed point multiplication at different register sizes n . We assume $N = 10k$ samples for the quantum rounding method. The resources estimated are for a fault-tolerant implementation of quantum rounding using the comparator method from Fig. 2. Descriptions of the three methods are given in the text. We see reductions in the number of gates and their depth for the quantum rounding approach. The number of qubits used is slightly worse for quantum rounding.

References

- [1] Thomas Alexander, Naoki Kanazawa, Daniel J Egger, Lauren Capelluto, Christopher J Wood, Ali Javadi-Abhari, and David C McKay. Qiskit pulse: programming quantum computers through the cloud with pulses. *Quantum Science and Technology*, 5(4):044006, 2020.
- [2] Matthew Amy, Dmitri Maslov, Michele Mosca, and Martin Roetteler. A meet-in-the-middle algorithm for fast synthesis of depth-optimal quantum circuits. *IEEE Transactions on Computer-Aided Design of Integrated Circuits and Systems*, 32(6):818–830, 2013.
- [3] Alex Bocharov, Martin Roetteler, and Krysta M. Svore. Efficient synthesis of universal repeat-until-success quantum circuits. *Phys. Rev. Lett.*, 114:080502, Feb 2015.
- [4] Shouvanik Chakrabarti, Andrew M. Childs, Tongyang Li, and Xiaodi Wu. Quantum algo-

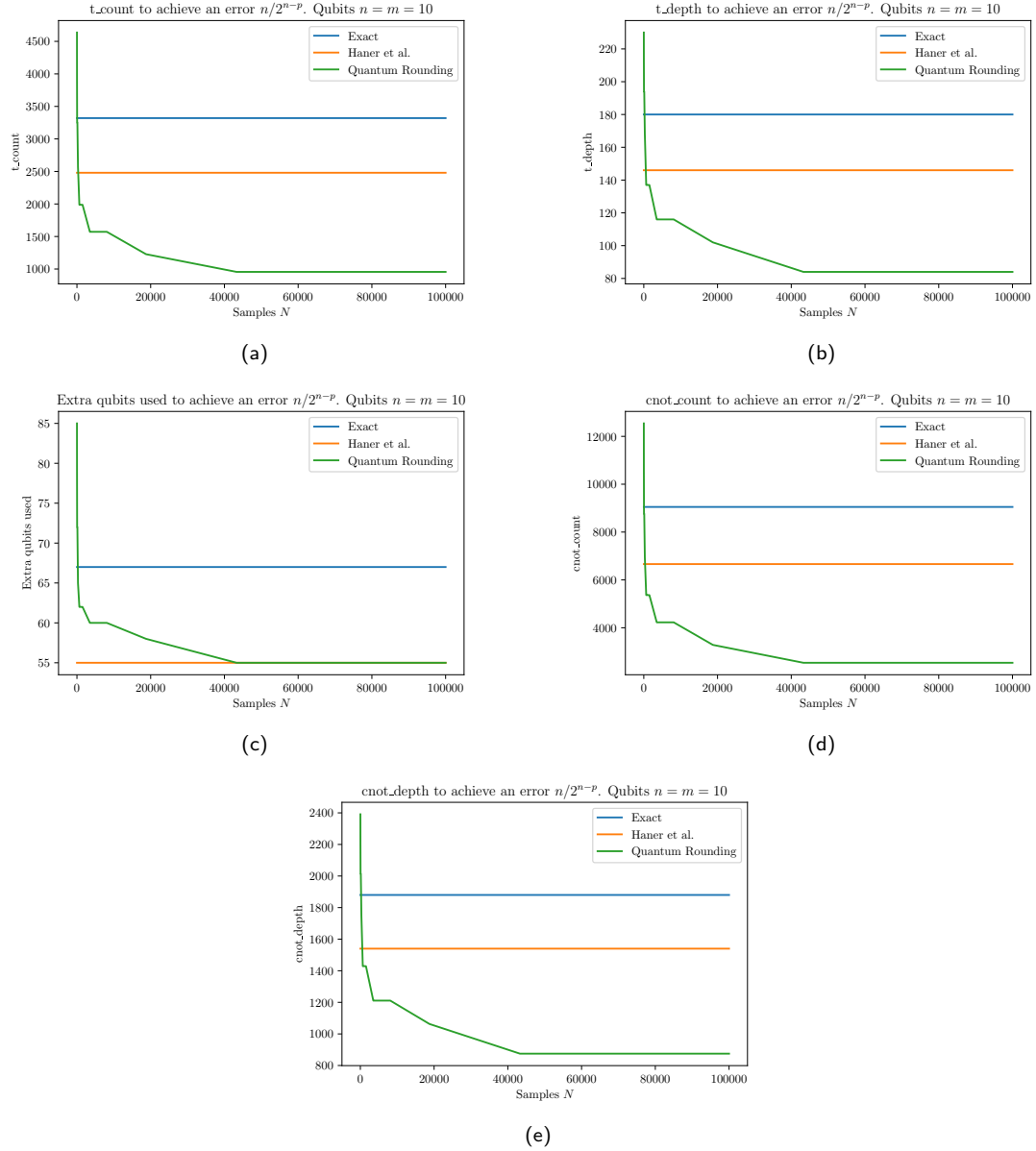


Figure 4: Comparison of different resource metrics for fixed point multiplication with a different number of samples N . We assume $n = 10$ -bit quantum registers. The resources estimated are for a fault-tolerant implementation of quantum rounding using the comparator method from Fig. 2. Descriptions of the three methods are given in the text. We see reductions in the number of gates and their depth for the quantum rounding approach. The number of qubits used is worse for quantum rounding when $N < 40k$. For larger N the qubit number becomes comparable. We see that the resource improvement from quantum rounding approaches a floor for N of approximately 50k samples in this case. For very small N (e.g. $N < 50$) quantum rounding is the worst method, but rapidly improves as the number of samples grows.

- rithms and lower bounds for convex optimization. *Quantum*, 4:221, January 2020.
- [5] Michael P Connolly, Nicholas J Higham, and Théo Mary. Stochastic rounding and its probabilistic backward error analysis. *SIAM Journal on Scientific Computing*, 43(1):A566–A585, 2021.
 - [6] Shantanu Debnath, Norbert M Linke, Caroline Figgatt, Kevin A Landsman, Kevin Wright, and Christopher Monroe. Demonstration of a small programmable quantum computer with atomic qubits. *Nature*, 536(7614):63–66, 2016.
 - [7] Thomas G. Draper, Samuel A. Kutin, Eric M. Rains, and Krysta M. Svore. A logarithmic-depth quantum carry-lookahead adder. *Quantum Info. Comput.*, 6(4):351–369, July 2006.
 - [8] Edward Farhi, Jeffrey Goldstone, and Sam Gutmann. A quantum approximate optimization algorithm. *arXiv preprint arXiv:1411.4028*, 2014.
 - [9] Vlad Gheorghiu and Michele Mosca. Benchmarking the quantum cryptanalysis of symmetric, public-key and hash-based cryptographic schemes. *arXiv preprint arXiv:1902.02332*, 2019.
 - [10] Craig Gidney and Martin Ekerå. How to factor 2048 bit rsa integers in 8 hours using 20 million noisy qubits. *arXiv preprint arXiv:1905.09749*, 2019.
 - [11] Thomas Häner, Martin Roetteler, and Krysta M Svore. Optimizing quantum circuits for arithmetic. *arXiv preprint arXiv:1805.12445*, 2018.
 - [12] Michael Hopkins, Mantas Mikaitis, Dave R Lester, and Steve Furber. Stochastic rounding and reduced-precision fixed-point arithmetic for solving neural ordinary differential equations. *Philosophical Transactions of the Royal Society A*, 378(2166):20190052, 2020.
 - [13] Cody Jones. Low-overhead constructions for the fault-tolerant toffoli gate. *Phys. Rev. A*, 87:022328, Feb 2013.
 - [14] Taewan Kim and Byung-Soo Choi. Efficient decomposition methods for controlled-r n using a single ancillary qubit. *Scientific Reports*, 8(1), 2018.
 - [15] Vadym Kliuchnikov, Dmitri Maslov, and Michele Mosca. Fast and efficient exact synthesis of single qubit unitaries generated by clifford and t gates, 2013.
 - [16] Guang Hao Low. Hamiltonian simulation with nearly optimal dependence on spectral norm. In *Proceedings of the 51st Annual ACM SIGACT Symposium on Theory of Computing*, STOC 2019, page 491–502, New York, NY, USA, 2019. Association for Computing Machinery.
 - [17] Dmitri Maslov. Basic circuit compilation techniques for an ion-trap quantum machine. *New Journal of Physics*, 19(2):023035, 2017.
 - [18] Dmitri Maslov and Mehdi Saeedi. Reversible circuit optimization via leaving the boolean domain. *IEEE Transactions on Computer-Aided Design of Integrated Circuits and Systems*, 30(6):806–816, 2011.
 - [19] Giulia Meuli, Mathias Soeken, Martin Roetteler, and Thomas Häner. Enabling accuracy-aware quantum compilers using symbolic resource estimation. *Proceedings of the ACM on Programming Languages*, 4(OOPSLA):1–26, 2020.
 - [20] Mantas Mikaitis. Stochastic rounding: Algorithms and hardware accelerator. *arXiv preprint arXiv:2001.01501*, 2020.
 - [21] David E Muller. Application of boolean algebra to switching circuit design and to error detection. *Transactions of the IRE professional group on electronic computers*, (3):6–12, 1954.
 - [22] Michael A. Nielsen and Isaac L. Chuang. *Quantum computation and quantum information*. Cambridge University Press, Cambridge ; New York, 10th anniversary ed edition, 2010.
 - [23] Patrick Rall. Faster coherent quantum algorithms for phase, energy, and amplitude estimation. *arXiv preprint arXiv:2103.09717*, 2021.
 - [24] IS REED. A class of multiple-error-correcting codes and the decoding scheme. *IRE Trans. Information Theory*, 4:38–49, 1954.
 - [25] Neil J Ross and Peter Selinger. Optimal ancilla-free clifford+ t approximation of z-rotations. *Quantum Information & Computation*, 16(11-12):901–953, 2016.
 - [26] Yasuhiro Takahashi, Seiichiro Tani, and Noboru Kunihiro. Quantum addition circuits and unbounded fan-out, 2009.
 - [27] Lu Xia, Martijn Anthonissen, Michiel Hochstenbach, and Barry Koren. Improved stochastic rounding. *arXiv preprint arXiv:2006.00489*, 2020.

A Quantum semi-rounding

In this section we introduce *quantum semi-rounding* to gain some of the benefits of quantum rounding but with potentially less quantum resources. In this variant, we only round the most significant bit of the remainder $\bar{x}_{m-1} \dots \bar{x}_0$. An example circuit for this is illustrated in Fig. 5, however other circuits may be used. In this method, we have no error when the remainder has a Hamming weight of one and have less error on other remainders. Quantum semi-rounding does not currently improve on the quantum rounding implementation with the comparator, but if there were to be an improved quantum circuit to identify the most significant bit in a register then it potentially could.

While quantum rounding improves the worst case error, quantum semi-rounding does not. The worst case error is the same as round-nearest where we consider only the most significant bit \bar{x}_{m-1} . However, the average case will be better. If we assume that we are rounding across uniformly distributed remainders then the average case error from rounding down is

$$\hat{\epsilon}_{RD} = \frac{1}{2^m} \sum_r r = \frac{1}{2^m} \sum_{j=0}^{2^m-1} \left(j \frac{\epsilon_{RD}}{2^m} \right) \quad (23)$$

$$= \frac{\epsilon_{RD}}{2^{m+1}} (2^m - 1). \quad (24)$$

For quantum semi-rounding we index the error contribution of each remainder based on the number k of left padding zeros. The uniform average case error for quantum semi-rounding (for $m \geq 2$) is given by

$$\hat{\epsilon}_{QSR} = \frac{1}{2^m} \sum_{k=1}^{m-1} \sum_{j=0}^{2^{m-k}-1} \left(j \frac{\epsilon_{RD}}{2^m} \right) \quad (25)$$

$$= \frac{\epsilon_{RD}}{3 \cdot 2^{2m+1}} (4^m - 3 \cdot 2^m + 2). \quad (26)$$

Their ratio is then

$$\frac{\hat{\epsilon}_{QSR}}{\hat{\epsilon}_{RD}} = \frac{1}{3 \cdot 2^m} (2^m - 2). \quad (27)$$

For large m this approaches an average case error improvement of 3X compared to conventional rounding methods. For small m we do better, with the $m = 2$ and $m = 3$ cases resulting in improvements of 6X and 4X respectively.

These values are the average case errors that quantum semi-rounding converges to in the limit of many samples. This contrasts with the quantum rounding case where the limit of large samples converges to zero error. Similarly we expect to converge with large N so that

$$\hat{\epsilon}_{QSR} \leq \mathcal{O} \left(\frac{\hat{\epsilon}_{RD} (2^m - 2)}{3 \cdot 2^m} + \frac{1}{\sqrt{N}} \right), \quad (28)$$

for a fixed probability of failure and a number of samples N .

A.1 Quantum semi-rounding with l most significant bits of the remainder

We can also extend the quantum-semi rounding method to determine the rotation angle based on the l most significant bits of the remainder instead of just the first. This can be done by performing the appropriate Boolean logic before each controlled rotation. The circuit to implement this is an extension of the one showed in Figure 5 (which depicts the case when $l = 1$) where we add the appropriate Toffoli gates and ancilla qubits to compute the aforementioned Boolean logic before each controlled rotation gate. The Toffoli-count and depth for this method increases exponentially with l and hence this extension may quickly become inefficient compared to the full quantum rounding method, e.g. for values $l > 3$. However, this method leads to an enhancement in the performance in the average case error. The goal is to find the first non-zero bit as we scan the remainder string from $|\bar{x}_{m-1}\rangle$ to $|\bar{x}_0\rangle$. To compute this, we start at Eq. (29) but instead of starting

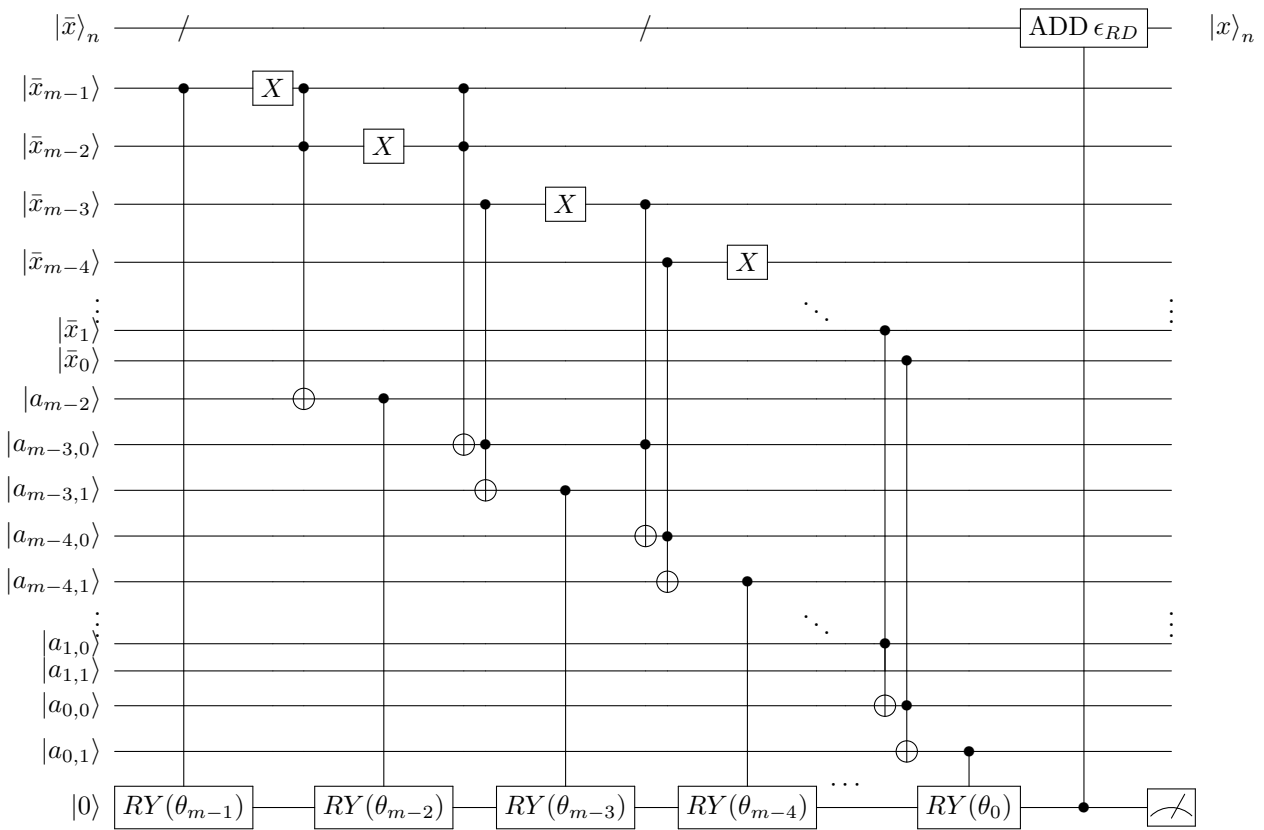


Figure 5: Circuit for quantum semi-rounding an $n + m$ -bit number $|\bar{x}\rangle$ to a n -bit number $|x\rangle_n$. Here $\theta_i = \sin^{-1}(2^{-(m-i)})$. The m -bit register becomes garbage that can be uncomputed. The ancilla can be conditionally reset and reused. The Boolean logic of the Toffoli gates means that each rotation $Ry(\theta_i)$ is only applied if \bar{x}_i is the most significant 1-bit in the m -bit register.

the second sum going from $j = 0$ to $j = 2^{m-k} - 1$, it goes from $j = 0$ to $j = 2^{m-k-l+1} - 1$ which gives us

$$\hat{\epsilon}_{QSR_l} = \frac{1}{2^m} \sum_{k=1}^{m-1} \sum_{j=0}^{2^{m-k-l+1}-1} \left(j \frac{\epsilon_{RD}}{2^m} \right) \quad (29)$$

$$= \frac{\epsilon_{RD}}{3 \cdot 2^{2m+l}} (2 \cdot 2^{2m-l} - 3 \cdot 2^m - 8 \cdot 2^{-l} + 6). \quad (30)$$

Following the same procedure as in the main text, we expect to converge to this error so that

$$\hat{\epsilon}_{QSR_l} \leq \mathcal{O} \left(\frac{\hat{\epsilon}_{RD} (2^{1-l}(2^{2m-l} + 3 \cdot 2^m + 2^{2m-l} + 6))}{3 \cdot (4^m - 2^m)} + \frac{1}{\sqrt{N}} \right), \quad (31)$$

for a fixed probability of failure and a number of samples N .

B Resource Estimation Framework

In this section we explicitly compute the resources that may be used to run the quantum rounding and quantum semi-rounding algorithms in both a fault-tolerant and NISQ setting.

B.1 Computing resources in a Fault-Tolerant setting

In a fault-tolerant setting, we assume that resources are dominated by the T gate count and depth, with the CNOT gate count and depth having a smaller but still non-trivial impact. Therefore we choose to use appropriate circuits that minimize the T-depth whilst still ensuring that our CNOT gate counts and depth does not become exponentially large. This last constraint comes from the fact that any Boolean function of n qubits can be constructed with $\mathcal{O}(\log(n))$ T-depth but $\mathcal{O}(2^n)$ CNOT gates and ancilla qubits, by decomposing the function using the Positive Polarity Reed-Muller expansion [24, 21] where the Boolean products of n variables can be done with T-depth $\log(n)$. However the quantum implementation of the XORs in the expansion requires a CNOT depth of $\mathcal{O}(2^n)$. In addition this construction also requires $\mathcal{O}(2^n)$ ancilla qubits. Therefore we explicitly avoid circuits that are constructed in this manner.

We use the following calculations:

- A single Toffoli gate has a T-count of 4, a T-depth of 1, a CNOT count and depth of 10 and uses 2 ancilla qubits which are uncomputed (from Figure 1 in [13]).
- The circuit we will use for the Ry rotations is the repeat-until-success one described in [3, 15]. When taking into account the probability of failure, this results in an average T-count and T-depth of $\lceil 1.149 \log_2(1/\epsilon) + 9.2 \rceil$ from [25] where ϵ is the precision of the rotation angle.
- The controlled- Ry rotation with the least T-depth can be found in [2, 14], which gives a T-count of $3 \times \lceil 1.149 \log_2(1/\epsilon) + 9.2 \rceil$, a T-depth of $\lceil 1.149 \log_2(1/\epsilon) + 9.2 \rceil$, a CNOT count and depth of 4 and an additional uncomputed ancilla qubit for a given error ϵ .
- The circuit to compare two registers has a Toffoli count of $6n - 2\lceil \log_2(n) \rceil - 4$, a Toffoli depth of $2\lceil \log_2(n) \rceil + 5$ with an additional $2n - 2$ CNOT count and 2 CNOT depth (from Table 1 in [7]).

B.2 Resources in a NISQ setting

In a NISQ setting, we treat Ry as a native gate.³ We focus on quantifying the 2-qubit and single-qubit gate counts and depths. Therefore, we choose the more NISQ suitable circuits for certain subroutines that reduce (e.g. minimize) the 2-qubit gate depth.

³In practice hardware may make available some other parameterized single-qubit rotation, but transforming between them may require only a small basis change.

| Resource | Quantum Rounding Fault-tolerant | NISQ |
|------------------------------|---------------------------------------|---------------------------------------|
| Total additional used qubits | $m + 1$ | $m + 1$ |
| Uncomputed ancilla qubits | $4m - \lceil \log_2 m \rceil - 2$ | $2m - \lceil \log_2 m \rceil - 2$ |
| T-count | $24m - 8\lceil \log_2 m \rceil - 16$ | - |
| T-depth | $2\lceil \log_2 m \rceil + 5$ | - |
| Two-qubit gate count | $62m - 20\lceil \log_2 m \rceil - 42$ | $32m - 10\lceil \log_2 m \rceil - 22$ |
| Two-qubit gate depth | $10\lceil \log_2 m \rceil + 27$ | $12\lceil \log_2 m \rceil + 32$ |
| Single-qubit gate count | - | $32m - 10\lceil \log_2 m \rceil - 22$ |
| Single-qubit gate depth | - | $10\lceil \log_2 m \rceil + 27$ |

Table 2: The resources used to load the remainder in the ancilla amplitude for quantum rounding given an m -qubit remainder register.

| Resource | Semi-rounding Fault-tolerant | NISQ |
|------------------------------|--|------------|
| Total additional used qubits | 1 | 1 |
| Uncomputed ancilla qubits | $2m - 2$ | $2m - 3$ |
| T-count | $36m + 3m\lceil 1.149 \log_2 \epsilon \rceil - 12$ | - |
| T-depth | $12m + \lceil 1.149m \log_2 \epsilon \rceil - 3$ | - |
| Two-qubit gate count | 20m-30 | $12m - 15$ |
| Two-qubit gate depth | 20m-30 | $12m - 15$ |
| Single-qubit gate count | - | $2m - 2$ |
| Single-qubit gate depth | - | $2m - 2$ |

Table 3: The resources used to load the remainder in the ancilla amplitude for quantum semi-rounding given an m -qubit remainder register with a maximum rotation bias error of ϵ .

- We treat controlled- Ry rotations as a single native 2-qubit gate [6, 17, 1].
- For Toffoli gates we use the circuit from Figure 4.8 in [22], which leads to a native 2-qubit gate count and depth of 5 and no single-qubit gates.
- The comparator circuit from [7] includes $2m - 2$ two-qubit gate count and 2 two-qubit gate depth in addition to the ones used to construct the Toffoli gates, as well as an additional $2m + 1$ single-qubit gate count and 2 single-qubit gate depth aside from the ones used to construct the Toffoli gates.

B.3 Resources for remainder loading

The first step of the quantum (semi-)rounding methods is to load the remainder into the amplitudes of the ancilla qubit. The resource estimates for this step in various rounding methods are given in Table 2 and Table 3. We have assumed a maximum rotation bias error of $\epsilon_B = 2^{-m}$.

B.4 Resources for the controlled addition gate

The controlled addition gate in the quantum (semi-)rounding circuits adds ϵ_{RD} to the quantum number $|\bar{x}\rangle$. We first discuss the resources used to implement the addition of a constant to a quantum register and then discuss how to add the control feature.

A quantum circuit for doing an in-place addition of two n -bit fixed-point numbers $a = a_{n-1}a_{n-2}\dots a_0$ and $b = b_{n-1}b_{n-2}\dots b_0$ stored in the registers $|a\rangle$ and $|b\rangle$ respectively can be found in Figure 5 in [7]. However, when a is a pre-determined classical constant, we can construct an efficient circuit with the following steps.

1. Construct a circuit to add 2 n -qubit registers $|a\rangle$ and $|b\rangle$ as described in [7].
2. Remove all gates that are controlled on qubits $|a_i\rangle$ where $a_i = 0$

| Resource | Fault-tolerant implementation |
|------------------------------|--|
| Total additional used qubits | 1 |
| Uncomputed ancilla qubits | $3n - \lfloor \log_2 n \rfloor + \sum_{i=1}^{\log_2 n} \lfloor \frac{n}{2^i} \rfloor - 5$ |
| T-count | $34n - 12 \lfloor \log_2 n \rfloor - 12 \lfloor \log_2 n - 1 \rfloor$ $+ 12 \sum_{i=1}^{\log_2 n} \lfloor \frac{n}{2^i} \rfloor$ $+ 12 \sum_{i=1}^{\log_2 n - 1} \lfloor \frac{n-1}{2^i} \rfloor - 12$ |
| T-depth | $\lfloor \log_2 n \rfloor + \lfloor \log_2 n - 1 \rfloor$ $+ \lfloor \log_2 \frac{n}{3} \rfloor + \lfloor \log_2 \frac{n-1}{3} \rfloor + 11$ |
| Two-qubit gate count | $77n - 30 \lfloor \log_2 n \rfloor - 30 \lfloor \log_2 n - 1 \rfloor$ $+ 30 \sum_{i=1}^{\log_2 n} \lfloor \frac{n}{2^i} \rfloor$ $+ 30 \sum_{i=1}^{\log_2 n - 1} \lfloor \frac{n-1}{2^i} \rfloor - 29$ |
| Two-qubit gate depth | $10 \lfloor \log_2 n \rfloor + 10 \lfloor \log_2 n - 1 \rfloor$ $+ 10 \lfloor \log_2 \frac{n}{3} \rfloor + 10 \lfloor \log_2 \frac{n-1}{3} \rfloor + 111$ |

Table 4: The resources used to perform a ctrl-add 1 to an n -qubit register using the fault-tolerant implementation.

| Resource | NISQ implementation |
|-------------------------------------|--|
| Total additional used qubits | 1 |
| Number of uncomputed ancilla qubits | $n - \lfloor \log_2 n \rfloor + \sum_{i=1}^{\log_2 n} \lfloor \frac{n}{2^i} \rfloor - 1$ |
| Two-qubit gate count | $\lceil 44.2n \rceil - 15 \lfloor \log_2 n \rfloor - 15 \lfloor \log_2 n - 1 \rfloor$ $+ 15 \sum_{i=1}^{\log_2 n} \lfloor \frac{n}{2^i} \rfloor$ $+ 15 \sum_{i=1}^{\log_2 n - 1} \lfloor \frac{n-1}{2^i} \rfloor - 14$ |
| Two-qubit gate depth | $5 \lfloor \log_2 n \rfloor + 5 \lfloor \log_2 n - 1 \rfloor$ $+ 5 \lfloor \log_2 \frac{n}{3} \rfloor$ $+ 5 \lfloor \log_2 \frac{n-1}{3} \rfloor + 56$ |
| Single-qubit gate count | $2n + 1$ |
| Single-qubit gate depth | 2 |

Table 5: The resources used to perform a ctrl-add 1 to an n -qubit register using the NISQ implementation.

3. Remove all gates that are controlled on the now un-altered $|0\rangle$ ancilla qubits
4. Remove any back-to-back X, CNOT or Toffoli gates (since they are self-adjoint)
5. Replace all the gates that are controlled on qubits $|a_j\rangle$ where $a_j = 1$ with their uncontrolled versions.
6. Remove the $|a\rangle$ quantum register.

For our particular circuits we want to implement the $ADD_{\epsilon_{RD}}$ gate where we replace $a_0 = 1$ and $a_i = 0$ for $i \neq 0$. This leads to a further reduction in resources used to construct this gate compared to the resources used to add 2 arbitrary n qubit registers as described in Section 4.2 in [7]. The T-count is reduced by 35% while the number of ancilla qubits remains the same. An example of a circuit to add 1 to a 10-qubit register can be seen in Figure 6.

Once we have constructed the $ADD_{\epsilon_{RD}}$ gate, we can turn it into a controlled- $ADD_{\epsilon_{RD}}$ gate by using the method shown in Figure 3 in [18]. This uses an additional n -qubit ancilla register, along with two sets of controlled swap gates. Each individual controlled swap gate comprises 3 Toffoli gates as seen in Figure 7. The resources used for a controlled $ADD_{\epsilon_{RD}}$ gate using this procedure are given in Table 4 and Table 5.

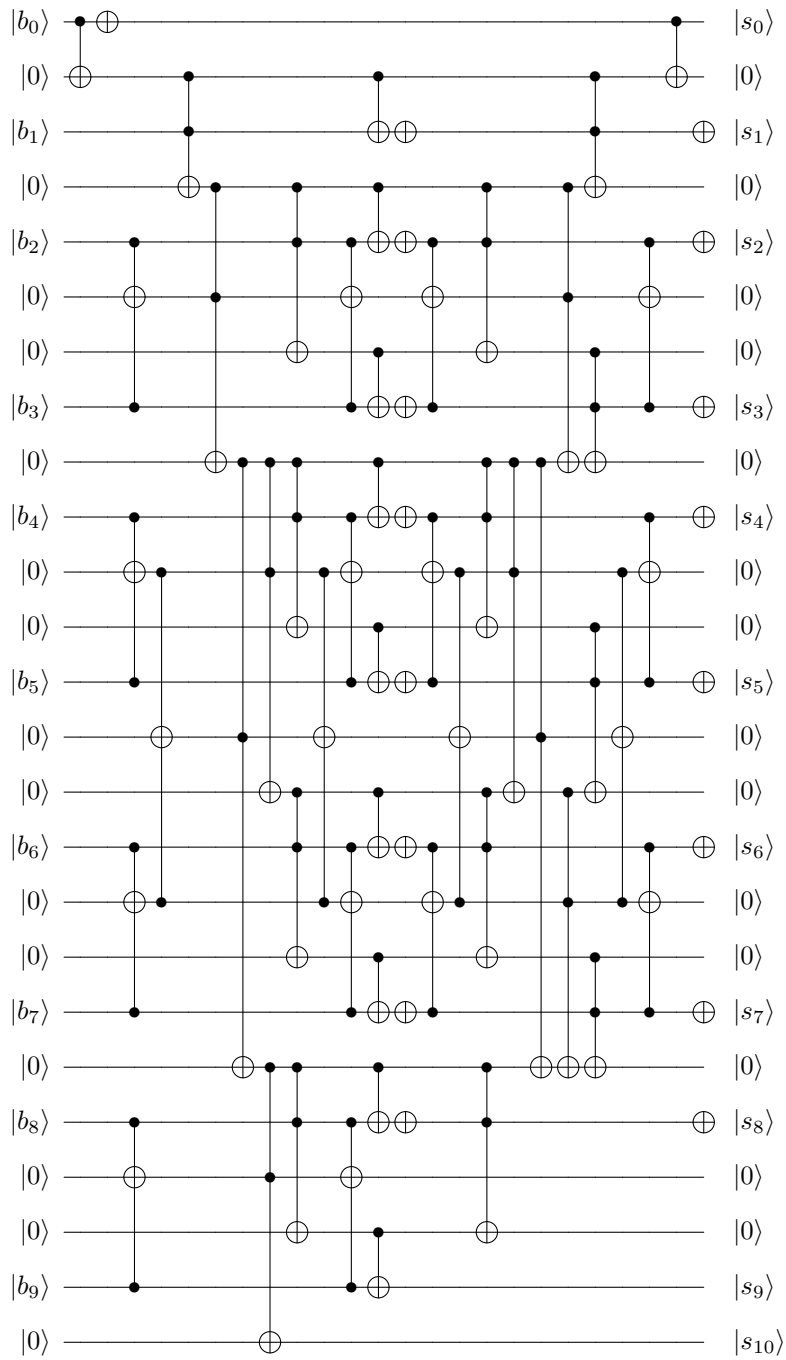


Figure 6: A circuit to add the constant ϵ_{RD} to a 10-qubit register. The circuit was constructed by taking the addition circuit from Figure 5 in [7] and performing the relevant modifications as described in Section B.4.

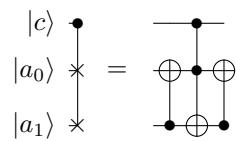


Figure 7: The decomposition of a controlled-swap gate into Toffoli and CNOT gates.

C Algorithm and resources for generalized fixed-point multiplication

In this section we consider the resources used to perform a fixed-point multiplication of two numbers a and b . We assume that they can be represented by the binary numbers

$$\begin{aligned} a &= a_{p_a} a_{p_a-1} \dots a_0 . a_{-1} \dots a_{p_a-n_a} \\ b &= b_{p_b} b_{p_b-1} \dots b_0 . b_{-1} \dots b_{p_b-n_b} \end{aligned}$$

and we will store them in two separate registers $|a\rangle$ and $|b\rangle$. In Appendix A in [11], the authors state that fixed point multiplication can be computed using a series of controlled additions e.g. initialize an output register $|00\dots 0\rangle$ and perform n_a ctrl-additions of $2^j \times b$ for j ranging from $p-n$ to p where each j th addition is controlled on a_j . In Appendix B of [11] the authors describe the T-count for the case where the two input registers and the output register have the same values for n and p , leading to the final result having a maximum error of $\frac{n}{2^{n-p}}$. We extend this original algorithm to be for any two distinct input register sizes and as a function of a desired error ϵ leading to an output register with size parameters n_{out} and p_{out} . We do this by first recognizing that the multiplication includes n_a separate control-additions to the output register e.g. one control-addition for each a_j term. The resources used to perform a control-addition are discussed in Section B.4. Naively we would use all the n_b bits in b for each addition. However, for a given error, we can use less than n_b bits in some of these additions. To compute this number, we start by noticing that given a total error of ϵ , this means that we can tolerate an error of up to $\frac{\epsilon}{n_a}$ for each controlled-addition. Each controlled-addition term will have the value $a_j \times 2^j$ times b . Therefore we may only use the f_j most significant ones for every a_j term, where f_j is computed by solving for $2^{p_b-f_j} \leq \frac{\epsilon}{n_a}$. For values of j for which $f_j > n_b$, we use all n_b bits. We note that the final output register size parameters will be

$$\begin{aligned} p_{out} &= p_a + p_b \\ n_{out} &= p_{out} - \log_2 \epsilon \end{aligned}$$

We finally note that the case of the Haner et al. [11] method is the special case where $\epsilon = \frac{n}{2^{n-p}}$, and the Exact method mentioned in the text (i.e. $\epsilon = 0$) is also a special case in which we end up performing n_a control-additions all with n_b bits registers.